

Supplementary materials

Title: Incremental metabolic benefits from cryoablation for paroxysmal atrial fibrillation: insights from metabolomic profiling

Brief Title: Metabolic benefits of cryoablation

Authors: Mengjie Xie, MD^{a,1}, Fuding Guo, MD^{a,1}, Jun Wang, MD^{a,1}, Yijun Wang, MD^a, Zhihao Liu MD^a, Jing Xie MD, PhD^a, Zhuo Wang MD, PhD^a, Songyun Wang MD, PhD^a, Liping Zhou, MD, PhD^a, Yueyi Wang, MD, PhD^a, Hong Jiang, MD, PhD^{a,*}, Lilei Yu, MD, PhD^{a,*}

Affiliation:

^a Department of Cardiology, Renmin Hospital of Wuhan University; Institute of Molecular Medicine, Renmin Hospital of Wuhan University; Hubei Key Laboratory of Autonomic Nervous System Modulation; Taikang Center for Life and Medical Sciences, Wuhan University; Cardiac Autonomic Nervous System Research Center of Wuhan University; Hubei Key Laboratory of Cardiology; Cardiovascular Research Institute, Wuhan University, Wuhan, 430060, P.R. China.

¹ **These authors contributed equally to this work.**

***Correspondence:**

Lilei Yu, MD, PhD, FACC, FESC

Department of Cardiology, Renmin Hospital of Wuhan University,
No.238 Jiefang Road, Wuhan City, Hubei Province 430060, P.R. China,
Tel: +86 27 88041911; Fax: +86 27 88040334,
E-mail: lileiyu@whu.edu.cn

Hong Jiang, MD, PhD, FACC

Department of Cardiology, Renmin Hospital of Wuhan University,

No. 238 Jiefang Road, Wuhan City, Hubei Province 430060, P.R. China,

Tel: +86 27 88041911; Fax: +86 27 88040334,

E-mail: hong-jiang@whu.edu.cn

Declaration of Interest

The authors declare no competing interests

Supplemental Table S1: Patient baseline characteristics (n=10)

Demographics

Age, yrs 60.0 ± 12.3

Male gender 6 (60)

Clinical status and history

LA diameter, cm 3.9 ± 0.5

LVEF, % 59.4 ± 1.8

Hypertension 3 (30)

Diabetes 0 (0)

CAD 0 (0)

CKD 0 (0)

Prior stroke or TIA 0 (0)

OSAS 1 (10)

Body mass index, kg/m² 25.7 ± 2.4CHA₂DS₂-Vasc score 1.9 ± 1.6

Data are mean ± SD or number (%) of patients. LA, left atrium; LVEF, left ventricular ejection fraction; CAD, coronary artery disease; CHF, chronic heart failure; CKD, chronic kidney disease; TIA, transient ischemic attack; OSAS, obstructive sleep apnea-hypopnea syndrome.

5

Supplemental Table S2: Index procedure characteristics (n=10)

Total procedure time, min 68.0 ± 14.0

Ablation time, min 48.6 ± 10.2

Fluoroscopy time, min	18.5 ± 5.6
Acute PV isolation	40/40(100)
Procedure-related complications	1 (5.6)

Data are mean ± SD or number (%) of patients.

Supplemental Table S3: Summary of differential metabolites to distinguish post-CRYO from pre-CRYO of AF patients.

Metabolites	KEGG.ID	RT	m/z	Platform	FC	p.value	VIP
Phenethylamine	C05332	3.427	121.0894	C18:pos	55.0731	0.0020	5.2148
Tyramine	C00483	0.953	137.0843	C18:pos	41.0491	0.0020	4.881
Oxymetazoline	C07363	7.305	260.189	C18:pos	20.6755	0.0020	4.3808
5-methoxydimethyltryptamine	C08309	5.148	218.1421	C18:pos	17.2322	0.0020	4.6211
Paracetamol	C06804	5.44	151.0636	C18:pos	17.0961	0.0020	4.2362
Hexobarbital	C11723	2.823	236.1158	C18:neg	13.7240	0.0020	3.1174
Psilocin	C08312	4.174	204.1265	C18:pos	9.3121	0.0020	4.4015
Anandamide (aea)	C11695	9.791	347.2824	C18:pos	4.1653	0.0020	2.5774
Palmitoleic acid	C08362	9.782	254.2242	C18:neg	3.6461	0.0020	2.404
8z,11z,14z-eicosatrienoic acid	C03242	10.084	306.2555	C18:neg	3.2491	0.0020	1.9254
8,11,14-Eicosatrienoylethanolamide	C13828	9.926	349.298	C18:pos	3.2346	0.0020	1.9528
Linoleic acid	C01595	9.929	280.2398	C18:neg	3.1038	0.0020	2.3767
Nitrendipine	C07713	4.329	360.1318	C18:neg	2.2021	0.0020	2.0735
Docosahexaenoic acid	C06429	9.837	328.24	C18:neg	2.1936	0.0020	1.4694

Pirenzepine	C07508	9.608	351.1707	C18:pos	2.1197	0.0020	1.7321
Anacardic acid	C10759	9.571	348.2663	C18:pos	1.6831	0.0020	1.2325
Emedastine	C07785	9.711	302.2096	C18:pos	1.4826	0.0020	1.5443
L-citrulline	C00327	0.685	175.096	C18:pos	0.7289	0.0020	1.1024
4-Glutathionyl cyclophosphamide	C11583	4.536	565.0931	C18:neg	0.7264	0.0020	1.0952
Ethyl butyrylacetate	C02975	5.661	158.0942	C18:neg	0.6876	0.0020	1.1196
5-hydroxyindoleacetate	C05635	3.467	191.0585	C18:pos	0.5394	0.0020	1.6756
11(z)-eicosenoic acid	C16526	10.742	310.2868	C18:neg	3.9632	0.0039	2.3948
11(z),14(z)-eicosadienoic acid	C16525	10.357	308.2712	C18:neg	3.6249	0.0039	2.2385
2-arachidonoyl glycerol	C13856	9.48	378.2771	C18:pos	2.7147	0.0039	1.9713
Oleoylethanolamide	C20792	9.606	325.298	C18:pos	2.4479	0.0039	1.7436
Quinoline	C06413	5.146	129.0581	C18:pos	0.6990	0.0039	1.0127
Decarbamoylsaxitoxin	C20021	7.145	256.1282	C18:neg	0.6864	0.0039	1.0434
Furfuranol	C20441	0.703	98.037	C18:pos	0.6779	0.0039	1.2412
Cyclohexylamine	C00571	3.382	99.105	C18:pos	0.6252	0.0039	1.336
5-(4-Acetoxybut-1-ynyl)-2,2'-bithiophene	C04485	0.606	276.0284	C18:neg	0.5716	0.0039	1.5497
Caprylic acid (octanoic acid)	C06423	7.391	144.1153	C18:pos	0.4827	0.0039	1.7959

P-cresol	C01468	3.819	108.0578	C18:pos	0.4821	0.0039	1.4975
Gentisic acid	C00628	3.527	154.0265	C18:neg	0.4540	0.0039	1.9145
Medroxyprogesterone	C07119	8.916	344.2348	C18:neg	0.2684	0.0039	2.7994
Cis-5,8,11,14,17-eicosapentaenoic acid	C06428	9.655	302.2243	C18:neg	2.3626	0.0059	1.5127
Myristic acid	C06424	9.661	228.2088	C18:neg	2.0894	0.0059	1.5328
D-erythro-sphingosine 1-phosphate	C06124	9.092	379.2488	C18:pos	0.7504	0.0059	1.0106
Testosterone glucuronide	C11134	8.759	464.239	C18:pos	0.6259	0.0059	1.3721
Saccharin	C12283	2.77	182.999	C18:neg	0.5870	0.0059	1.8861
(9cis)-retinal	C16681	8.915	284.214	C18:pos	0.2323	0.0059	2.7157
Lignocaine	C07073	4.092	234.1734	C18:pos	0.1780	0.0059	4.3383
2-hydroxyhippuric acid	C07588	3.397	195.053	C18:neg	0.0299	0.0059	1.4764
Capsi-amide	C17515	10.091	269.272	C18:pos	1.9216	0.0098	1.3531
Arachidonic acid	C00219	9.683	304.2402	C18:pos	1.5713	0.0098	1.0314
Fumaric acid	C00122	0.621	116.011	C18:neg	0.7587	0.0098	1.1527
D-ornithine	C00515	0.591	132.0901	C18:pos	0.7335	0.0098	1.0903
Leucine	C00123	1.776	131.0949	C18:pos	0.6840	0.0098	1.3403
Hydroxyzine	C07045	7.372	374.1753	C18:pos	0.4888	0.0098	1.6137

Caprolactam	C06593	3.643	113.0843	C18:pos	0.3340	0.0098	2.0215
Tartronic acid	C02287	0.619	120.0059	C18:neg	1.7957	0.0137	1.6217
Tridemorph	C11285	9.805	297.3032	C18:pos	1.5040	0.0137	1.0497
Taurine	C00245	0.651	125.0146	C18:neg	0.7385	0.0137	1.1061
Cholic acid	C00695	8.289	408.2872	C18:neg	0.5138	0.0137	1.6666
Glycerin	C00116	0.703	92.0476	C18:pos	2.5919	0.0195	1.5862
(+/-)12(13)-dihome	C14829	8.241	314.2453	C18:neg	1.7376	0.0195	1.5143
Bilirubin	C00486	7.275	584.2641	C18:pos	1.6813	0.0195	1.2496
Glycine	C00037	4.18	75.0322	C18:pos	1.4188	0.0195	1.159
(-)-secoisolariciresinol	C18167	9.336	362.1736	C18:neg	1.3746	0.0195	1.0283
1-palmitoylglycerone 3-phosphate	C01192	9.364	408.2274	C18:neg	0.6144	0.0195	1.7782
Trimethylamine n-oxide	C01104	0.676	75.0687	C18:pos	0.4377	0.0195	1.598
Quercitrin	C01750	5.172	448.1007	C18:pos	0.3094	0.0195	1.1704
Rabeprazole	C07864	5.199	359.1304	C18:pos	0.0041	0.0195	1.8773
Diloxanide furoate	C07637	3.379	327.008	C18:neg	5.2621	0.0273	1.7016
Pyridoxal	C00250	3.964	167.0586	C18:pos	2.0986	0.0273	1.7157
Ecgonine	C10858	2.724	185.1055	C18:pos	1.8253	0.0273	1.1197

Fmet	C03145	1.616	177.0459	C18:neg	1.5077	0.0273	1.2528
Glycodeoxycholic acid	C05464	8.451	449.3136	C18:neg	0.3951	0.0273	1.3177
Alfentanil	C08005	8.718	416.2541	C18:pos	0.3331	0.0273	1.931
Dihydroxyindole	C05578	4.003	149.048	C18:pos	3.3752	0.0371	3.895
L-theanine	C01047	1.169	174.1008	C18:pos	1.9969	0.0371	1.0327
Amide c18	C13846	9.888	283.2874	C18:pos	1.5792	0.0371	1.039
Gamma-aminobutyric acid	C00334	0.702	103.0635	C18:pos	1.3606	0.0371	1.0394
Ginkgoic acid	C10794	9.069	346.2504	C18:neg	0.4972	0.0371	1.4952
Thromboxane b2	C05963	6.908	370.2353	C18:neg	0.4494	0.0371	1.7306
Steviol	C20212	8.703	318.2191	C18:neg	0.3119	0.0371	2.513
Retinoate	C00777	8.692	300.2089	C18:pos	0.2981	0.0371	1.8614
beta-alanine	C00099	0.697	89.0477	C18:neg	1.3674	0.0488	1.0534
Deoxycholic acid	C04483	7.705	392.2924	C18:neg	0.4995	0.0488	1.1987
Mono(2-ethylhexyl) phthalate (mehp)	C03343	7.904	278.1514	C18:neg	0.4879	0.0488	2.0141

Supplemental Table S4: Pathway analysis from KEGG in pre- and post-CRYO AF patients.

Pathway	Count	pvalue	p.adjust	geneID
Biosynthesis of unsaturated fatty acids	7	3.47E-06	0.0005	C03242/C16525/C16526/C06428/C06429/C00219/C01595
Retrograde endocannabinoid signaling	5	0.0002	0.0121	C00219/C00334/C00116/C13856/C11695
Neuroactive ligand-receptor interaction	8	0.0003	0.0136	C00245/C00099/C00334/C00483/C00037/C06124/C13856/C11695
Thermogenesis	3	0.0022	0.0728	C00116/C13856/C11695
Linoleic acid metabolism	4	0.0033	0.0890	C03242/C14829/C00219/C01595
Fatty acid biosynthesis	3	0.0079	0.1759	C06424/C08362/C06423
Fc gamma R-mediated phagocytosis	2	0.0172	0.2853	C00219/C06124
Retinol metabolism	2	0.0172	0.2853	C00777/C16681
Methane metabolism	3	0.0326	0.3944	C01104/C00483/C00037
Primary bile acid biosynthesis	3	0.0326	0.3944	C00245/C00695/C00037
Serotonergic synapse	3	0.0326	0.3944	C05963/C00219/C05635

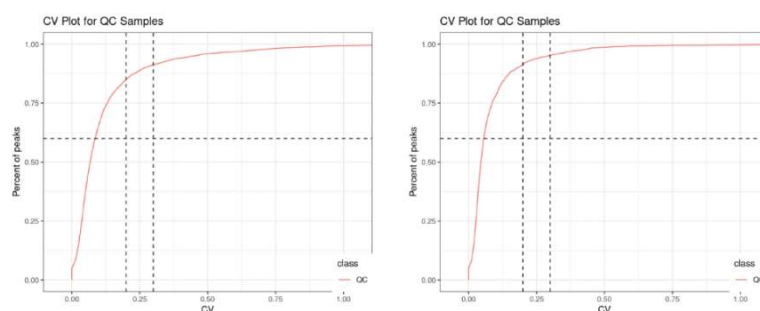
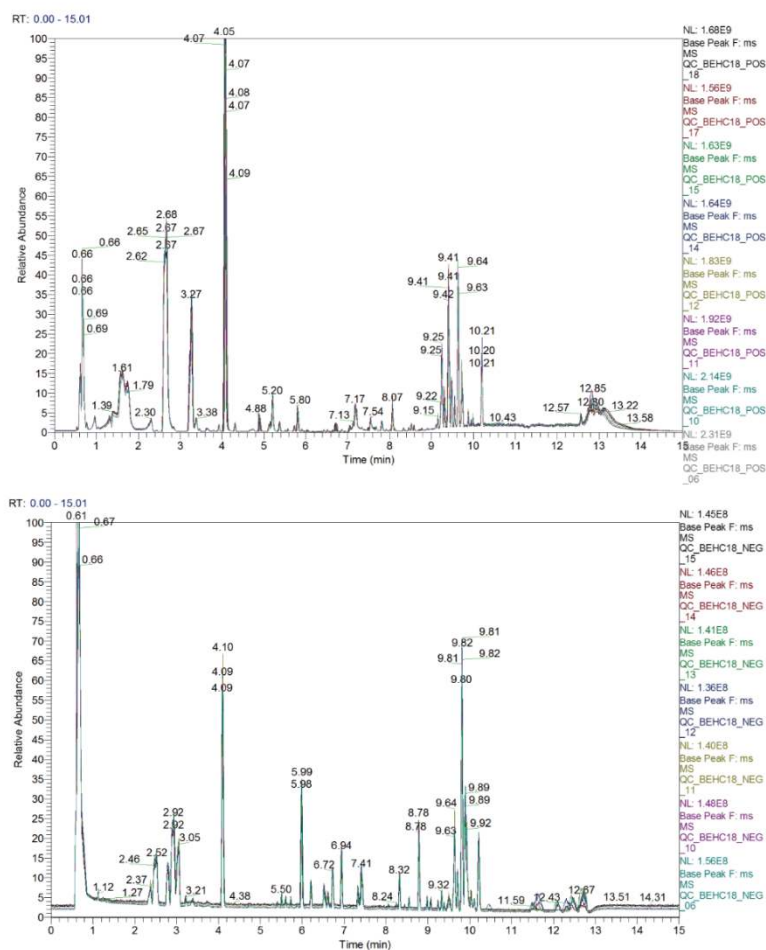
A**B**

Figure S1 Data preprocessing and quality control. (A) CV distribution plot for all QC samples. CV of the relative peak area in all samples were calculated in positive modes (left) and negative modes (right), and compounds with CV greater than 30% were deleted. (B) BPC overlay of QC samples. The BPC (base peak chromatogram) of all QC samples were overlapped, the spectrum overlap was good, and the retention time and peak response intensity fluctuated little. Upper is in positive modes, and lower is in negative mode.

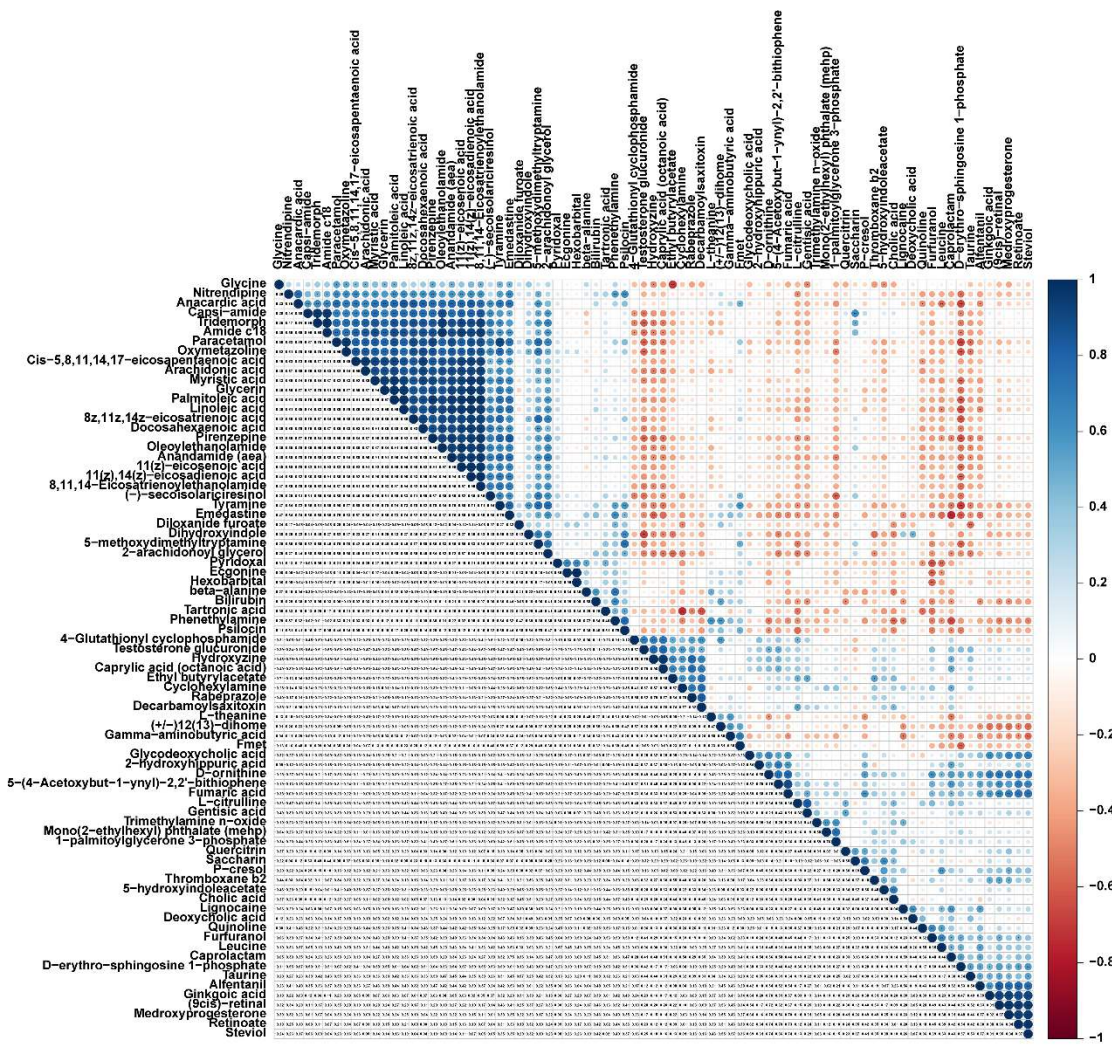


Figure S2 Correlation analysis among all differential metabolites after CRYO. Correlation analysis among all 79 differential metabolites. Pearson correlation coefficients between pairs of compounds are shown in the lower left corners of the panels. In the upper right corners, the degree of correlation and p values are shown for each pair. Red and blue indicate negative and positive correlations, respectively. *p < 0.05; **p < 0.01.

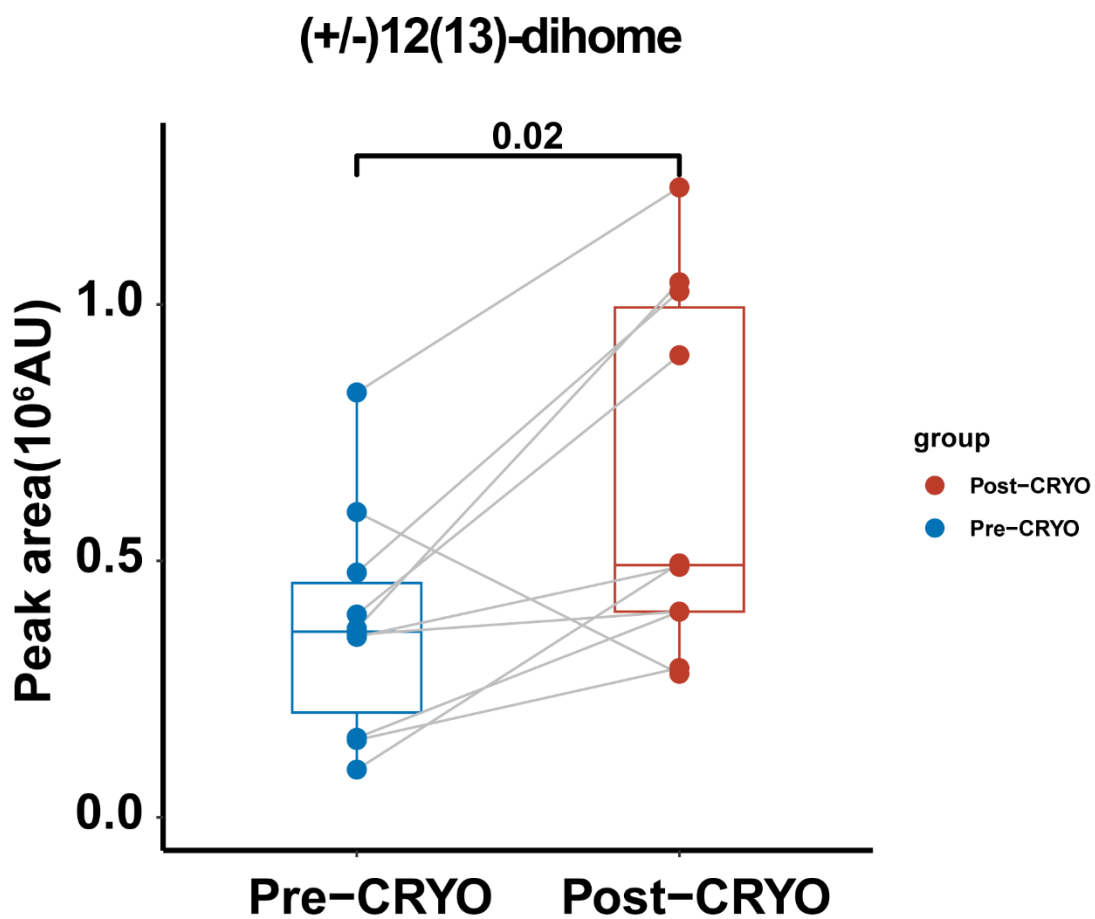


Figure S3 Abundance of (+/-)12(13)-dihome in Pre- and Post- CRYO groups. Paired Wilcoxon signed-rank test was used for comparisons between sampling sites, Values represented mean \pm SD.

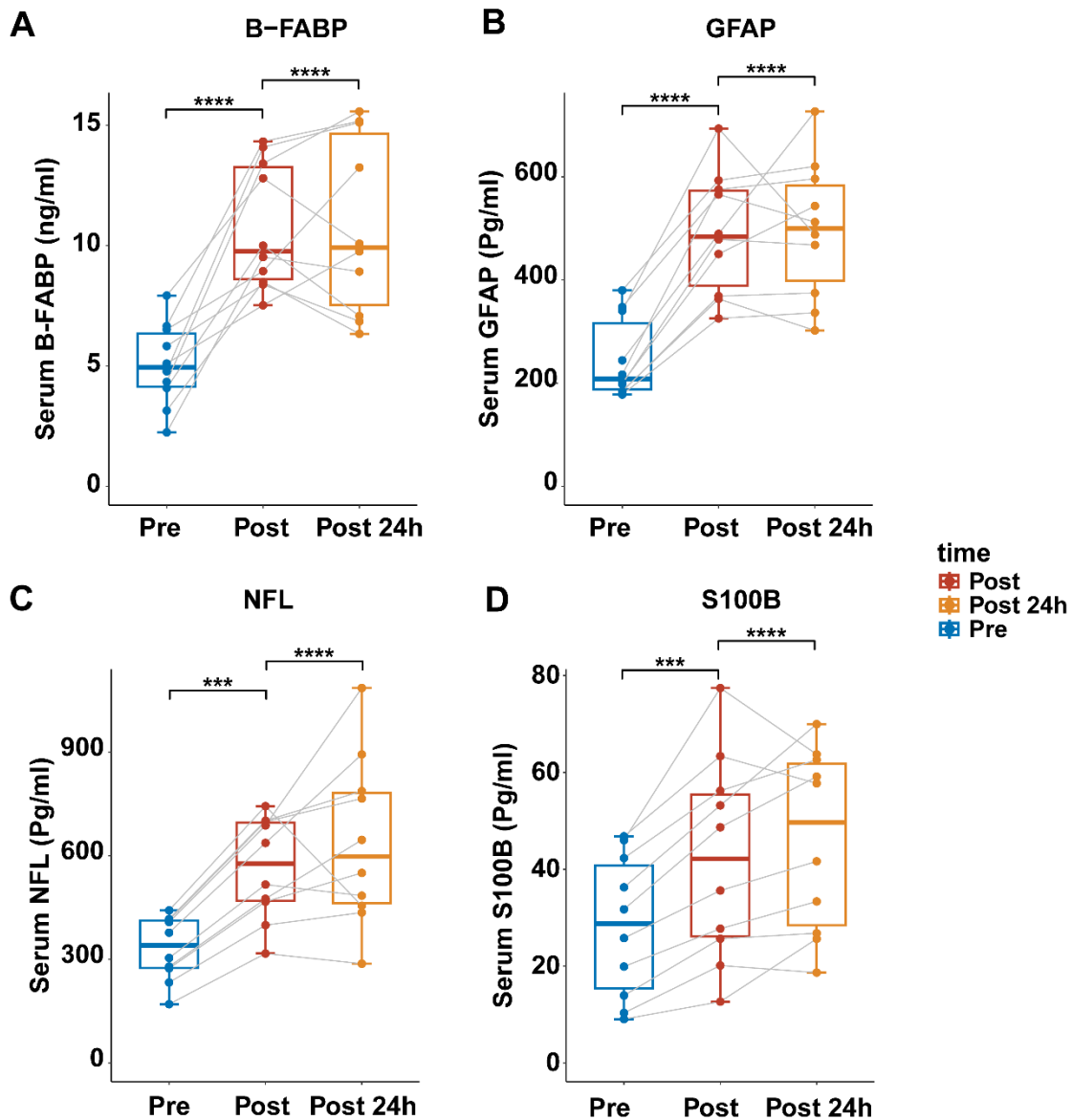


Figure S4 Changes in nerve injury biomarkers in patients after CRYO ablation. (A) B-FABP levels, (B) GFAP levels, (C) NFL levels and (D) S100B levels were measured before, after and 24h after CRYO catheter-based treatment of AF, n=10. B-FABP, brain fatty acid-binding protein; GFAP, glial fibrillary acidic protein; NFL, serum neurofilament light; S100B, S-100 protein beta chain. (****P < 0.0001, ***P < 0.001; paired one-way ANOVA analysis with Tukey's multiple comparisons test was used for statistical analysis. Values represented mean \pm SD).

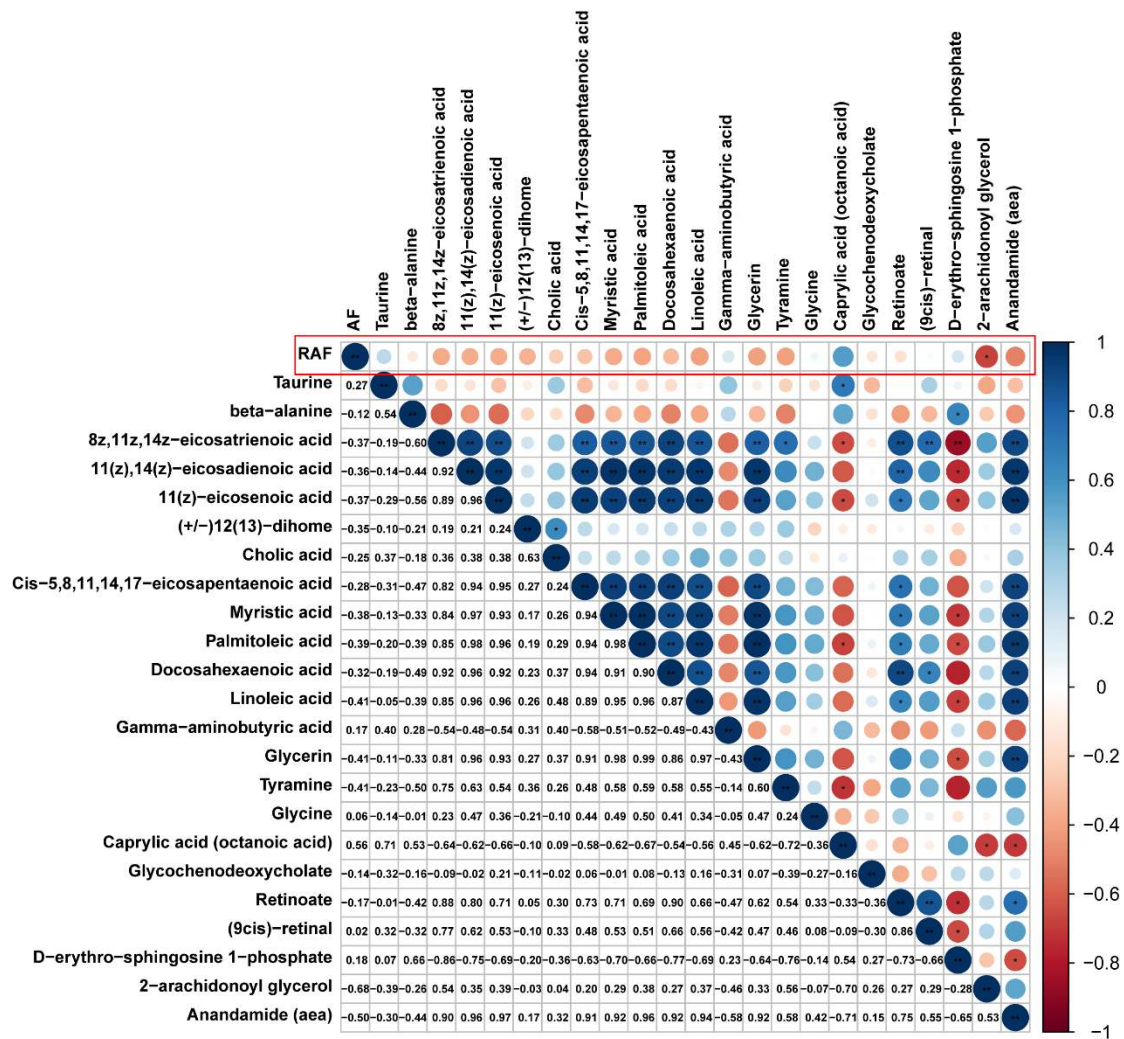


Figure S5 Correlation analysis between altered metabolites and recurrent AF after CRYO.

Pearson correlation coefficients between pairs of compounds after CRYO are shown in the lower left corners of the panels. In the upper right corners, the degree of correlation and p values are shown for each pair. Red and blue indicate negative and positive correlations, respectively.

20

* $p < 0.05$; ** $p < 0.01$.

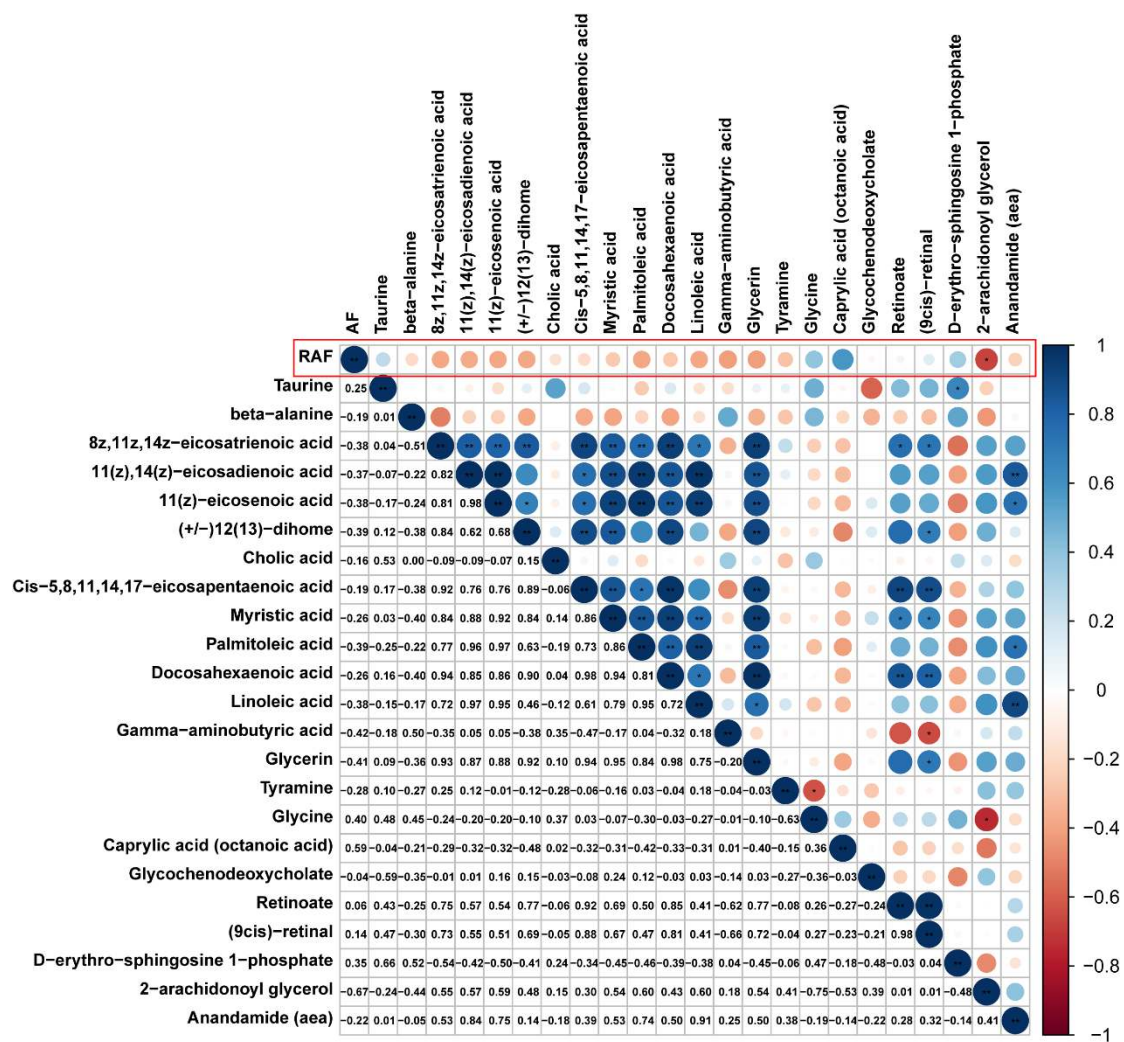


Figure S6 Correlation analysis between relative level of altered metabolites and recurrent AF. Pearson correlation coefficients between pairs of relative level of altered metabolites are shown in the lower left corners of the panels. In the upper right corners, the degree of correlation and p values are shown for each pair. Red and blue indicate negative and positive correlations, respectively. * $p < 0.05$; ** $p < 0.01$.

25